Microbial dynamics in an intertrappean lake during the terminal phase of Deccan volcanism

Yogaraj Banerjee[1,2]*, Prosenjit Ghosh[1], K. Sajeev[1], Shrinivas G. Viladkar[3]

[1]Centre for Earth Sciences, Indian Institute of Science, Bangalore, India

[2]STARLAB, Department of Earth and Atmospheric Sciences, Central Michigan University, MI, USA

[3]Department of Earth and Environmental Sciences, Indian Institute of Science and Education Research, Bhopal, India

*Corresponding author: Yogaraj Banerjee (ybanerjee15@gmail.com)

Abstract: Biogeochemical changes associated with Deccan volcanism and their potential link to the K/Pg extinction event are still debated in Palaeoclimate research. Contemporary terrestrial organosedimentary deposits are important archives for understanding the perturbation in the biogeochemical cycling during this critical episode in Earth's history. Here, we report an intertrappean lacustrine carbonate deposit from the Amba Dongar region in the northwestern part of the Deccan igneous province, formed during the terminal phase of Deccan volcanism. This sedimentary horizon contains two types of biologically induced carbonate deposits: (1) older Type I (fine and discontinuous laminae with uneven boundaries) and younger Type II (thick and regular laminae with well-defined boundaries). Our sedimentological and stable isotope investigation captures evidence of gradual eutrophication of the lake system associated with the Deccan volcanism. Based on the clumped isotope-based temperature estimates (33°-41°C), we propose a "hot and sour soup"-like condition promoting microbial carbonate precipitation.

Keywords: Deccan, K/Pg extinction, Cretaceous, Microbial, Eutrophication, Lacustrine.

1.Introduction:

The Deccan traps represent a major continental flood basalt volcanism covering ~2 million Km^3 area – the longest lava flows on Earth (Font et al., 2016; Fendley et al; 2019; Keller et al., 2009; Tandon 2002). Studies suggest different phases of Deccan volcanic eruptions, while the main eruption took place around 66 Ma within a short time span (< 1 Ma or even less) close to the K/Pg boundary (Renne et al, 2015; Schone et al., 2015; Self et al., 2022 and references therein). It was estimated that around $4.14*10^{17}$ mol CO_2 was released into the atmosphere during Deccan volcanism (Jay and Widdowson 2008; Tobin et al., 2017). The sudden increase in atmospheric CO_2 concentrations and other gases due to the volcanism was considered to have played a key role in driving the K/Pg extinction event (Zhang et al., 2018; Ray and

Ramesh, 1999). On the contrary, several studies have suggested that Deccan volcanism played a minor role in extinction (Chiarenza et al., 2020; Dzombak et al., 2020). Terrestrial organo-sedimentary deposits provide valuable information about the cause (volcanism) and effect (biogeochemical changes) relationships during critical events in Earth history. In the context of Deccan volcanism, intertrappean sedimentary records have shown potential as important archives for deciphering late Cretaceous terrestrial hydrological cycles (Ghosh et al., 2006). In this study, we identified an intertrappean lacustrine sedimentary deposit from the Amba Dongar region, Western India. The Amba Dongar region is well-studied as a carbonatite ring dyke complex representing the late phase of Deccan volcanism (Viladkar 2015 and references therein). For the first time, we report an intertrappean lake system between the basaltic and carbonatite lava flows from the Amba Dongar region. The intertrappean sedimentary horizon studied in this project provides critical documentation of bioinduced carbonate precipitation during the magmatism as seen in the modern-day African continent, where carbonatite magmatism is underway, analogues to the Deccan volcanic eruption at the Amba Dongar region (Figure 1). This intertrappean lake system, with the excess presence of alkaline conditions, was conducive for primitive oxygenic life to survive and grow during the final phase of Deccan volcanism. We documented two types of lacustrine carbonates capturing varying growth conditions at different stages of the lake evolution associated with the sequence of volcanic events. We used a combination of stable isotope techniques in carbonates and microscopic imaging of rock structures to reach a conclusion about the dynamic trophic level of the lake ecosystem at the terminal stage of Deccan volcanism.

2.Geological settings:

Amba Dongar carbonatite-alkaline complex has been a longstanding subject of interest for geoscientists as it is one of the best examples of a carbonatite ring dike complex emplaced in the western part of the Deccan Flood Basalts (Fosu et al., 2020 and references therein). Over the last several decades, most of the studies from this region were related to the understanding of the origin, age and evolution of carbonatite magmatism (e.g., Viladkar 1981; Ray et al., 2003; Simonetti et al., 1995; Singh et al., 2022; Banerjee and Chakrabarti 2019; Fosu et al., 2019,2020, 2021; Chandra et al., 2018; Srivastava 1997; Samal et al., 2021,).

Geological, petrological and mineralogical investigations from the Amba Dongar region revealed the following sequence of events of intrusive volcanism (Viladkar and Sorkhtina 2021 and the references therein): (1) nephelinites and phonolites → (2) carbonatite breccia → (3) coarse-grained calcite carbonatite → (4) fine-grained calcite carbonatite dykes in sandstone, basalts and carbonatite breccia → (5) ankerite carbonatite dykes and plugs within the calcite carbonatites → (6) thin veins of sideritic carbonatite in the ankerite carbonatite → (7) fenitisation of sandstones → (8) the final hydrothermal phase of fluorite mineralization. The carbonatite complex intrudes Bagh sandstone and limestone and the Deccan traps sequence. U-Pb apatite radiometric age revealed ages 62±22 and 63±19 Ma for carbonatites and 62.3 ±1.6 Ma for nephelinites, representing the late-stage magmatic event during Deccan volcanism (Fosu et al., 2019). Here, we report an unnoticed intertrappean sedimentary deposits lying within the Deccan trap basalt and the carbonatite body at the northwestern periphery (near Mongra village) of the domal Amba Dongar complex, recording a coeval terrestrial biogeochemical change associated with CO_2 outgassing and large-scale carbonatite magmatism.

3. Description of the carbonate body:

The sedimentary strata investigated in this study displayed a stratiform macrostructure with well-defined laminae. Hand specimens and thick sections of the carbonate show alternate dark and light-coloured laminations (Supplementary Figures S1 and S2). The light and dark-colored rhythmic alterations comprise carbonate and siliciclastic material. Based on the nature of the lamination, the limestone deposit can be divided into two categories:

Type I: This type of carbonate is characterized by mm to micrometre-scale alternate bands of dark and light-coloured materials. We carried out 3D scanning of a 2.5x 2.5 cm block of this type of carbonate to reconstruct the lamina profile at 4X resolution (Supplementary Figure S3A). The tomographic image shows a wavy, gently convex laminae profile with undulatory boundaries in between. Regarding lateral continuity, most of the laminae are continuous, while some are irregularly spaced.

Type II: This type of carbonate is characterized by cm-scale alternate bands of dark and light-colored materials. A 3D tomographic reconstruction shows the presence of microbial chips (Supplementary Figure S3B). Petrographic investigation shows the presence of ooid structures in the Type II carbonates (Supplementary Figure S6), which showed microbial affinity. The BSE image shows detrital zircon grains (Supplementary Fig S4), which are bought by stream action, as evident from their rounded grain boundary, which demonstrates erosion and shape transformation before being incorporated in the carbonate matrix.

A BSE study using a Tescon integrated mineral analyzer (TIMA) shows the presence of mineral phases like Calcite, Albite, Othoclase, Wollastonite, Actinolite, Oligoclase, Ilmenite, Magnetite, and Apatite in the microbialite sample (Supplementary Fig. S5). The presence of Wollastonite adjacent to Calcite indicates contact metamorphism overprinting the microbialite structure in the laminated carbonate.

4. Methodology:

4.1 $\delta^{13}C$, $\delta^{18}O$ and Δ_{47} analyses of carbonates: Polished sample slabs were cleaned with DI water and treated with 30% H_2O_2 for 12 hours at room temperature to remove organic contaminants and then dried in a hot air oven at 60°C to remove the moisture. Sample powders from these slabs were drilled out from the white bands using microdrill. To determine the stable $\delta^{13}C$ and $\delta^{18}O$ of carbonate, we have followed the floating boat method as described in

Rangarajan et al. 2021; the methodology followed for analysis, including sample-standard bracketing, is similar to other studies (Ghosh et al., 2021 and Banerjee et al., 2023). In this method, pyrex glass boats loaded with 50 ugs of carbonate powder are placed in a glass vial prefilled with 1 ml of 105% phosphoric acid. Then, these loaded vials were flushed with He (99.99%) at 100 ml/min flow 1 rate. It was followed by acid digestion of carbonate samples for a duration of 70 minutes in a water bath, maintained at a constant temperature of 70°C. Analyses were carried out using a Thermo MAT 252 mass spectrometer housed at the stable isotope laboratory at the Indian Institute of Science, Bangalore, India. Samples were bracketed with Carrara marble (MARJ1: $\delta^{13}C$ value 1.96% and $\delta^{18}O$ -2.01‰) reference material (Rangarajan et al., 2021; Ghosh et al., 2005). The reproducibility of $\delta^{18}O$ and $\delta^{13}C$ were 0.04 and 0.05‰, respectively, based on replicate analysis of the reference carbonates.

We have carried out clumped isotope analysis on the bulk samples. For the acid digestions of carbonates at 25°C, we used a break-seal method, as discussed in detail in Fosu et al., 2019. As the CO_2 yield was less, we analyzed the samples at a relatively low voltage (at 6kV). The isotopic measurement was carried out at the Stable isotope laboratory at the Indian Institute of Science, Bangalore, using a Thermo MAT 253 mass spectrometer. From the Δ_{47} values, the temperature was obtained using a set of separate thermometry equations given by Ghosh et al. (2006); Zaarur et al. (2013); Petersen et al. (2019). We have used the temperature derived from Zaarur et al. (2013) equation for the interpretation and discussions since the acid digestion was done at 25°C. From the obtained temperature and $\delta^{18}O_{carbonate}$ information we calculated $\delta^{18}O_{water}$ using Kim and O'Neil 1997 equation.

4.2 $\delta^{13}C_{org}$ analysis: To determine the carbon isotopic compositions of the bulk organic matter, samples were leached for the presence of inorganic carbonate fraction using 20% HCl, and the remaining organic fraction was rinsed with de-ionized water and kept in an oven (70 °C) overnight for drying. The protocol for the isotopic investigation is described in Kaushal et al., 2019 and Paul et al., 2020. Around 170–180 µg of the dried sample powder was weighed and packed inside tin capsules and analyzed using elemental analyzer FLASH 2000 (Thermo Scientific) coupled with Conflo and isotope ratio mass spectrometer (IRMS) Delta V Advantage (Thermo Scientific, Bremen) at the stable isotope laboratory, Indian Institute of Science, Bangalore. Duplicate analyses of the samples were carried out to assign average values and understand the heterogeneity of the isotopic composition. The results are expressed as delta (δ) values per mil (‰) with respect to the Vienna Pee Dee Belemnite (VPDB) standard. Samples were bracketed with IAEA certified primary reference material, IAEA-CH-6, and in-house laboratory working reference materials, Oasis_Glucose (δ^{13}CVPDB = − 10.99 ± 0.03‰) and Oasis_Rice 1 (δ^{13}CVPDB = − 27.67 ± 0.04‰) for the isotopic investigation.

5. Discussions:

5.1 Stable carbon and oxygen isotopic composition:

For Type I carbonate, δ^{13}C values varies in range, from -2.24 to -5.54‰, with an average value of -3.76‰; δ^{18}O values varies in range from -1.43 to -8.10‰, with an average value of -4.31‰. For Type II carbonate, δ^{13}C values varies in range, from -5.34 to -9.05‰ with an average value of -7.09‰; δ^{18}O values varies in range, from -13.87‰ to -22.95‰ with an average value of -20.85‰ (Figures 2 and 3A).

Here, we compared our observation (Figure 2) with other available carbonate stable isotope compositions from late Cretaceous calcareous lithofacies recorded in the surrounding Narmada valley (Tandon et al., 1995 and Tandon and Andrews, 2001). The δ^{13}C and δ^{18}O values of palustrine limestone from the Saugar sub-region vary from -9.63‰ to -7.22‰ and -7.24‰ to -4.77‰, respectively. Intertrappean limestone beds registered δ^{13}C values -10.72‰ to-9.4‰ and δ^{18}O values -7.46‰ to -12.55‰. Nodular marine Bagh bed limestone recorded a range in δ^{13}C values from 1.97‰ to 0.74‰, while it is characterized by a broad spectrum of δ^{18}O values from -5.24‰ to -20.67‰. The microbial carbonates investigated here are isotopically distinct from the Proterozoic Vindhyan carbonates (Gilleaudeau et al., 2018; Banerjee et al., 2007). We have selected some of the carbonates from Type II carbonates and, leached out the carbonate fraction and carried out the $\delta^{13}C_{org}$ analysis on them. These samples also registered a strong relationship (Supplementary Figure S8) between $\delta^{13}C_{org}$ and $\delta^{13}C_{carb}$, indicating a greater carbon isotopic discrimination in carbonate relative to organic matter in an elevated aqueous CO_2-rich environment. Our study suggests that CO_2 released from the decomposition of organic matter was the source of carbon. This was incorporated into the inorganic carbonate deposited as a microbial mat.

5.2 Binary mixing of carbon:

The intertrappean lake would have had dissolved inorganic and organic carbon reservoirs similar to the modern-day volcanic lakes (Godfrey et al., 2021). Microbial carbonate precipitation captures a close coupling of two different carbon pools. We have carried out a two-component mixing model to determine the relative contribution of each of these pools to the carbonate precipitation in a close lacustrine system. In our model, we have used the following end members:

F1 (inorganic carbonate pool): the most enriched $\delta^{13}C$ composition of the carbonatite as reported in Fosu et al., 2019.

F2 (organic carbon pool): the most depleted $\delta^{13}C_{org}$ composition as documented in the present study.

We have assumed the $\delta^{13}C$ composition of the Cretaceous microbially mediated lacustrine carbonate is driven by the differential mixing of the carbon coming from these two different reservoirs.

$F_{ir} + F_{or} = 1$

F_{ir} = fraction of mixture from inorganic carbonate reservoir source

F or= fraction of mixture from organic carbon reservoir

F ir = (δM-δor)/(δir-δor)

δM= mean isotopic signature of the mixture (e.g., $\delta^{13}C$)

δor= isotopic signature of the organic carbon reservoir source

δir= isotopic signature of the inorganic carbonate reservoir source.

For Type I carbonate, the relative contribution from the inorganic fraction (F1) varies from 83.7 to 95.5% with an average of 90.1% (Figure 3B). The contribution of the organic carbon fraction varies from 4.5% to 16.3% with an average of 10%. For Type II carbonate, the contribution from F1 varies from 71.2% to 84.4%, with an average of 78.1%. The contribution of the organic carbon fraction varies from 15.6% to 28.2%, with an average of 21.9%. The increment in the relative proportion of the organic component in the Type II carbonate compared to the Type I was driven by the eutrophication of the lake ecosystem, which is justified based on the covariance of $\delta^{13}C$ and $\delta^{18}O$ values.

5.3 Isotopic depletion in $\delta^{18}O$:

As discussed in the previous section, Type II carbonates captured lighter $\delta^{13}C$ and $\delta^{18}O$ values than Type I carbonates. In this section, we explore the possible mechanism for this isotopic depletion in Type II carbonates.

We have documented similarities in the stable isotopic compositions of Type II carbonates and the primary igneous carbonates (PIC). Some of the values also match with post-carbonatite volcanic tuff deposit's stable isotopic composition (Viladkar et al., 2005). These observations lead to the following questions: What was the origin of these rocks (igneous vs sedimentary)? What caused the isotopic depletion in Type II carbonates than the Type I? All the field evidence, hand specimen and petrographic investigations in tandem with $\delta^{13}C_{org}$ values indicate an authigenic sedimentary origin of the carbonates investigated in the present study. Thus, there must be some other mechanism controlling the above-mentioned isotopic depletion, as discussed in the following section.

(a) The carbonatite and the Deccan basalt intruded the marine Bagh bed carbonates, which are much older than the lacustrine carbonates probed in the present study. During the basaltic and carbonatite volcanism, a certain amount of degassing would have happened from the underlying Bagh bed carbonate, which would have released lighter carbons. It could lead to the isotopic depletion in the $\delta^{13}C$ values during the precipitation of the lacustrine carbonates. In order to test this, we carried out additional stable isotope analysis of travertine samples that formed subsequent to the updoming of the Bagh limestone bed during the Deccan volcanic eruption events (Viladkar, 1981, Galwani et al.,1993). These travertines are older than the lacustrine carbonates. The $\delta^{13}C$ values of the travertine (Supplementary Figure S7) were more depleted than the Type I and II lacustrine carbonates. There is no systematic trend for the change in $\delta^{13}C$ values from Travertine → Type I carbonate → Type II carbonate according to their chronology of formation. It indicates that the degassing of older Bagh bed carbonates might not be the sole controller of the isotopic signatures of the lacustrine carbonates. Based on the petrographic evidence on the possible microbial origin of rocks and, a high correlation between $\delta^{13}C_{org}$ and $\delta^{13}C_{carbonate}$ values, we propose that microbial respiration played a significant role in controlling the isotopic values of the lacustrine carbonate deposits.

(b) Observations from modern-day highly eutrophic lakes show oxygen isotope disequilibrium in calcite precipitation during high productivity events, causing $\delta^{18}O$ depletion (Apolinarska et al., 2021; Fronval et al., 1995; Jinglu et al., 2004). In order to understand the involvement of possible disequilibrium effects, we examined the $\delta^{13}C$- $\delta^{18}O$ variability in both the types of carbonates. We document no significant correlation in Type I carbonates, while Type II carbonates exhibit a significant correlation (Figure 3A) , similar to that of some modern eutrophic lake systems (Supplementary Figure S9). This indicates two distinct phases of carbonate precipitation driven by the primary productivity in lake system adjacent volcanic conduit feeding carbonate rich magma and rainwater flow contributing nutrient for the eutrophication to happen.

Previous studies (Usdowski et al. 1991; Usdowski and Hoefs 1993) showed that pH plays an important role in controlling oxygen isotope fractionation factors between aqueous CO_2 , H_2CO_3 , HCO_3^-, and CO_3^{-2}, with respect to H_2O. At high pH conditions, hydroxylation of CO_2 ($CO_2+OH^- \leftrightarrow CO3^{-2}$) is more dominant than hydration of CO_2 ($CO_2+H_2O \leftrightarrow H^++HCO3^-$). Changes in the availability of CO_3^{-2} in surface water in tandem with an increase in primary productivity affect the carbonate-water oxygen isotope fractionation, leading to lighter $\delta^{18}O$ signature in carbonate.

In the case of the present study, increased precipitation after basaltic eruption enhanced nutrient supply to the lacustrine system through runoff. Enhanced nutrient supply could increase primary productivity and inhibit the growth of calcite. During this stage, Type I carbonate precipitated with thinner lamina thickness, higher $\delta^{13}C$ and $\delta^{18}O$ values, and a higher proportion of inorganic carbon fraction. As this stage continued, the available nutrients were consumed by the algal productivity. In the next stage, bio-induced calcification with changing pH conditions caused calcite precipitation at an accelerated rate. Type II carbonate with higher lamina thickness precipitated during this stage and thus captured signatures of isotopic disequilibrium and depleted $\delta^{18}O$ values.

5.4 Temperature and $\delta^{18}O$ water variability retrieved from clumped isotopes:

Our Δ_{47} based temperature reconstruction yielded a range between 33-41°C(±4°C) for the Type I carbonate. The obtained temperature values fall within the temperature range for the palaeoproterozoic carbonate mud associated with stromatolites (Banerjee et al., 2023). One of the Type II samples registered 38°C, similar to that of the Type I samples. However, another sample (Type II) retrieved from a zone near the contact metamorphism registered a higher temperature (60°C), indicating possible hydrothermal alteration. From the estimated temperature range, we hypothesized a "hot and sour soup" like condition in the lacustrine systems harnessing microbial life as the Deccan volcanism reached its terminal phase.

Reconstructed $\delta^{18}O_{water}$ varies from -2.03‰ to -4.14‰ for the Type I carbonate. Type II carbonate captured a much-depleted signature -16‰, indicating enhanced freshwater in the lake system. A triple oxygen isotope-based investigation also captured a $\delta^{18}O_{water}$ signature as low as -12‰, driven by intensified regional precipitation during the late Cretaceous (Ghoshmaulik et al., 2023). Extreme rainfall could be one of the possible reasons for such isotopic depletion, as documented in the Type II carbonate. Our previous investigations also captured isotopic fingerprints of possible storm events under elevated CO_2 scenarios causing abrupt isotopic depletion (Ghosh et al., 2018, Banerjee and Ghosh, 2024).

In summary, our preliminary clumped isotope investigation on bulk samples suggests a warm temperature range of 33-41°C for the investigated late Cretaceous lacustrine system. The $\delta^{18}O_{water}$ composition captures extreme depletion driven by intense precipitation. More high-resolution clumped isotope analysis will depict seasonal hydroclimate variability over the region.

5.5 Model scenario for the carbonate deposition:

Based on the field evidence, microscopic, mineralogical, and stable isotope investigation, we propose a model scenario (Figure 4) that explains the different stages of lake formation.

Stage I: In the first stage, basalt eruption associated with the Deccan volcanism occurred, which overlies the Bagh sandstone and limestones. This resulted in an updoming and development of dome-saddle-type undulatory topographic features in the terrain.

Stage II: It is well documented that Deccan volcanism intensified precipitation over the Indian subcontinent during the late Cretaceous (Ghosh et al., 2006, 2016; Ghoshmaulik et al., 2023). Such intense precipitation events would have created small lacustrine bodies in the low-lying (saddle) basins.

Stage III: In the next phase, runoff from volcanic geysers started bringing nutrients to newly formed small lakes. Type I carbonate started precipitating during this stage of high productivity, as registered by higher $\delta^{13}C$ values. The high-temperature environmental condition is supported by the inflow of DIC with a heavier composition similar to Bagh bed carbonate as a precursor. Alternate laminae with irregular boundaries are features developed in these carbonates. Such post-eruptive high-energy conditions could be documented in the present-day Tonga volcanic island (Liu and Tang, 2022), situated close to 30°S - the palaeolatitude for the Indian landmass during the late Cretaceous and also during Late Quaternary hydrological changes in Lake Natron -Magadi (Kenya), close to Olego lengai (Casanova and Hillaire MC, 2001).

Stage IV: The following stage was marked by algal blooms in the lake, which caused eutrophication. Bio-induced calcification resulted in the deposition of Type II carbonate with isotopic enrichment in organic matter, denoting viable pCO_2 condition. Rapid calcification yielded thicker laminae with depleted $\delta^{18}O$ values, as discussed in the previous section.

Stage V: This stage witnessed the phase of carbonatite magmatism. The contact between Type II microbial carbonate and carbonatite body carries the signatures of Wollastonite formation at the zone of contact metamorphism (Supplementary Figure S5). Viladkar et al. 2001 also reported the presence of subaqueous tufa in small lacustrine bodies after the carbonatite volcanism in the Amba Dongar region.

5.5 Implications for the life underneath the Deccan:

Recent investigations (Dutta et al., 2018; Bose et al., 2020; Mandal et al., 2022 and Sahu et al., 2022) focused on the characterization of microbial diversity and function through scientific deep drilling project at Koyna provided valuable insights into deep biosphere hosted within 65Ma Deccan basalt and Archean granitic basement. However, the origin of these microbial populations thriving in the deep subsurface is enigmatic.

A number of studies have reported the abundance of aquatic and semiaquatic flora in nutrient-rich palaeolakes from the Deccan volcanic province (Samant et al., 2020[a,b]; Samant et al., 2022; Khosla et al., 2022). For example , fossils of aquatic and semiaquatic flora, such as algae (Pediastrum, Lecaniella), dinocysts (Pierceites deccanensis), diatoms (Aulacoseira), aquatic ferns of Salvi niaceae (Azolla), Marsileaceae (Crybelosporites), and pollen grains of Sparganiaceae/Typhaceae (Sparga niaceaepollenites) were found near the Jamsavli section from the central India (Samant et al., 2022). Different fossilized diatom taxa were found in the Bagwanya palaeolake section (Samant et al., 2020[b]). Charophyte algae were reported from the Jhilimili intertrappean beds (Khosla et al., 2022). We hypothesize that the intertrappean lakes are the cradles of nutrient-rich soup that potentially seeded life into the dark, narrow passage of the Deccan subsurface. Our geochemical investigations and fossil evidence from intertrappean lakes from other localities (Samant et al., 2022) suggest these water bodies were rich in microbes. These nutrient and organic-rich fluids might have percolated through the fractures and seepages of the tectonically active region and reached the deeper parts of the crust. It would have contributed to promoting life in the deep biosphere in three ways (Figure 5):

(a) These fluids might have brought new microbial life forms to the deeper crust through fractures and faults (Templeton and Caro, 2023), gradually adopting the local environment and enriching biodiversity.

(b) The nutrient supply by these fluids might have fed and reactivated (Rajala and Bomberg, 2017) the pre-existed dormant cells of the deeper biosphere.

(c) Microbes could have moved towards nutrient-rich percolating fluids using their flagella and germinated in a favorable environment.

Further geomicrobiological and geochemical investigations on surface exposures, as well as subsurface intertrappean horizons and culture experiments, will elucidate more insights into the microbial response to the changing physicochemical condition during extinction events.

6. Conclusions:

This study documented microbial carbonates deposited in a lacustrine intertrappean sedimentary horizon from the Amba Dongar region, India. Based on the laminae thickness and stratigraphic positions, they are of two district types, representing two generations of carbonates. Stable carbon and oxygen isotope investigations on the carbonate and bulk organic matter of these rocks revealed syngenetic growth of microbial carbonate in association with organic matter as an algal colony in a eutrophic lake similar to modern-day lake system African continent adjacent to an active carbonatite body near Oldonyo lengai. Clumped isotope study reveals "hot and sour soup" like condition with 33-41°C temperature range promoted the microbially induced carbonate precipitation. Our study suggests a potential link between nutrient-rich intertrappean beds within the Deccan trap and its resemblance with the deep life form detected within drill core samples from the Koyna region.

Acknowledgement: We thank the Department of Science and Technology (DST), Government of India, and the Ministry of Earth Science, Government of India, for funding support.

Table 1| Results from carbonate clumped isotope investigation

	$\delta^{13}C$ (‰VPDB)	$\delta^{18}O$ (‰VPDB)	Δ_{47} (‰)	Temperature (°C) Equation 1	Temperature (°C) Equation 2	Temperature (°C) Equation 3	$\delta^{18}O_{water}$ (‰VSMOW)
Type I carbonate							
Sample 1	-3.73	-8.10	0.67	33.04±2	33.80±2	31.75±2	-4.14±0.5
Sample 2	-3.96	-7.50	0.64	41.10±4	40.86±4	43.49±4	-2.03±0.8
Sample 3	-4.12	-6.95	0.66	35.66±2	36.10±2	35.51±2	-2.49±0.5
Type II carbonate							
Sample 1	-7.62	-21.64	0.65	38.34±2	38.45±2	39.43±2	-16.75±0.5
Sample 2[#]	-5.4	-18.2	0.57	62.71±4	59.42±4	77.22±4	-9.14±0.8

Temperature was reconstructed using three different thermometry equations: Equation 1 (Zaarur et al., 2013); Equation 2 (Ghosh et al., 2006) and Equation 3 (Petersen et al., 2019).

$\delta^{18}O$ was calculated from the obtained temperature (equation 1) and $\delta^{18}O_{carbonate}$ information using Kim and O'Neil 1997 equation.

Hydrothermally altered sample.

References:

Apolinarska, K., Pleskot, K., Pełechata, A., Migdałek, M., & Pełechaty, M. (2021). Seasonal deposition of authigenic calcite out of isotopic equilibrium with DIC and water, and implications for paleolimnological studies. *Journal of Paleolimnology*, *66*(1), 41-53.

Banerjee, A., & Chakrabarti, R. (2019). A geochemical and Nd, Sr and stable Ca isotopic study of carbonatites and associated silicate rocks from the~ 65 Ma old Ambadongar carbonatite complex and the Phenai Mata igneous complex, Gujarat, India: Implications for crustal contamination, carbonate recycling, hydrothermal alteration and source-mantle mineralogy. *Lithos*, *326*, 572-585.

Banerjee, S., Ghosh, P., Banerjee, Y., & Riding, R. (2023). Oxygen isotopic composition of Paleoproterozoic seawater revealed by clumped isotope analysis of dolomite, Vempalle formation, Cuddapah, India. Chemical Geology, 621, 121356

Banerjee, S., Bhattacharya, S. K., & Sarkar, S. (2007). Carbon and oxygen isotopic variations in peritidal stromatolite cycles, Paleoproterozoic Kajrahat Limestone, Vindhyan basin of central India. *Journal of Asian Earth Sciences*, *29*(5-6), 823-831.

Banerjee, Y., & Ghosh, P. (2024). Freshwater plume-like condition near the north-eastern coastal Arabian Sea during early Miocene: Evidence from the stable isotope record in the growth bands of gastropods (Turritella sp.). *Terra Nova*.

Bose, H., Dutta, A., Roy, A., Gupta, A., Mukhopadhyay, S., Mohapatra, B., ... & Sar, P. (2020). Microbial diversity of drilling fluids from 3000 m deep Koyna pilot borehole provides insights into the deep biosphere of continental earth crust. *Scientific Drilling*, *27*, 1-23.

Casanova, J., & Hillare-Marcel, C. (1993). Carbon and oxygen isotopes in African lacustrine stromatolites: palaeohydrological interpretation. *Geophysical Monograph Series*, *78*, 123-133.

Chandra, J., Paul, D., Viladkar, S. G., & Sensarma, S. (2018). Origin of the Amba Dongar carbonatite complex, India and its possible linkage with the Deccan Large Igneous Province. *Geological Society of London Special Publication,* 493.

Chiarenza, A. A., Farnsworth, A., Mannion, P. D., Lunt, D. J., Valdes, P. J., Morgan, J. V., & Allison, P. A. (2020). Asteroid impact, not volcanism, caused the end-Cretaceous dinosaur extinction. *Proceedings of the National Academy of Sciences*, *117*(29), 17084-17093.

Dutta, A., Dutta Gupta, S., Gupta, A., Sarkar, J., Roy, S., Mukherjee, A., & Sar, P. (2018). Exploration of deep terrestrial subsurface microbiome in Late Cretaceous Deccan traps and underlying Archean basement, India. *Scientific reports*, *8*(1), 17459.

Dzombak, R. M., Sheldon, N. D., Mohabey, D. M., & Samant, B. (2020). Stable climate in India during Deccan volcanism suggests limited influence on K–Pg extinction. *Gondwana Research*, *85*, 19-31.

Fendley, I. M., Mittal, T., Sprain, C. J., Marvin-DiPasquale, M., Tobin, T. S., & Renne, P. R. (2019). Constraints on the volume and rate of Deccan Traps flood basalt eruptions using a combination of high-resolution terrestrial mercury records and geochemical box models. *Earth and Planetary Science Letters*, *524*, 115721.

Font, E., Adatte, T., Sial, A. N., de Lacerda, L. D., Keller, G., & Punekar, J. (2016). Mercury anomaly, Deccan volcanism, and the end-Cretaceous mass extinction. *Geology*, *44*(2), 171-174.

Fosu, B. R., Ghosh, P., & Viladkar, S. G. (2020). Clumped isotope geochemistry of carbonatites in the north-western Deccan igneous province: Aspects of evolution, post-depositional alteration and mineralisation. *Geochimica et Cosmochimica Acta*, *274*, 118-135.

Fosu, B. R., Ghosh, P., Chew, D. M., & Viladkar, S. G. (2019). Composition and U—Pb ages of apatite in the Amba Dongar Carbonatite–alkaline complex, India. *Geological Journal*, *54*(6), 3438-3454.

Fosu, B. R., Ghosh, P., Mishra, D., Banerjee, Y., K, P., & Sarkar, A. (2019). Acid digestion of carbonates using break seal method for clumped isotope analysis. *Rapid Communications in Mass Spectrometry*, *33*(2), 203-214.

Fosu, B. R., Ghosh, P., Weisenberger, T. B., Spürgin, S., & Viladkar, S. G. (2021). A triple oxygen isotope perspective on the origin, evolution, and diagenetic alteration of carbonatites. *Geochimica et Cosmochimica Acta*, *299*, 52-68.

Fronval, T., Bo Jensen, N., & Buchardt, B. (1995). Oxygen isotope disequilibrium precipitation of calcite in Lake Arresø, Denmark. *Geology*, *23*(5), 463-466.

Gilleaudeau, G. J., Sahoo, S. K., Kah, L. C., Henderson, M. A., & Kaufman, A. J. (2018). Proterozoic carbonates of the Vindhyan Basin, India: Chemostratigraphy and diagenesis. *Gondwana Research*, *57*, 10-25.

Ghosh, P., Adkins, J., Affek, H., Balta, B., Guo, W., Schauble, E.A., Schrag, D., Eiler, J.M., 2006. 13C-18O bonds in carbonate minerals: A new kind of paleothermometer. Geochim. Cosmochim. Acta 70, 1439–1456.

Ghosh, P., Patecki, M., Rothe, M., & Brand, W. A. (2005). Calcite- CO_2 mixed into CO_2- free air: A new CO_2- in- air stable isotope ref erence material for the VPDB scale. Rapid Communications in Mass Spectrometry: An International Journal Devoted to the Rapid Dissemination of up- to- the- Minute Research in Mass Spectrometry, 19(8), 1097–1119.

Ghosh, P., Prasanna, K., Banerjee, Y., Williams, I. S., Gagan, M. K., Chaudhuri, A., & Suwas, S. (2018). Rainfall seasonality on the Indian subcontinent during the cretaceous greenhouse. Scientific Reports, 8(1), 1–9.

Ghosh, P., Ramdas, L., Banerjee, Y., Thamizharasan, S., & Banerjee, S. (2021). Seasonal freshwater flux estimation using mollusc from the tropical Mandovi Zuari estuary, Goa, India. Journal of Earth System Science, 130(2), 107.

Ghosh, P., Sayeed, M. R. G., Islam, R., & Hundekari, S. M. (2006). Inter-basaltic clay (bole bed) horizons from Deccan traps of India: Implications for palaeo-weathering and palaeo-climate during Deccan volcanism. *Palaeogeography, Palaeoclimatology, Palaeoecology*, *242*(1-2), 90-109.

Ghosh, Prosenjit, Mikhail V. Vasiliev, Parthasarathi Ghosh, Soumen Sarkar, Sampa Ghosh, Keita Yamada, Yuichiro Ueno, Naohiro Yoshida, and Christopher J. Poulsen. (2016). "Tracking the migration of the Indian continent using the carbonate clumped isotope technique on Phanerozoic soil carbonates." *Scientific Reports* 6, 1,22187.

Ghoshmaulik, S., Bhattacharya, S. K., Hazra, M., Roy, P., Khan, M. A., Liang, M. C., ... & Sarkar, A. (2023). Triple oxygen isotopes in intertrappean fossil woods: Evidence of higher tropical rainfall during Deccan volcanism. *Chemical Geology*, *634*, 121599.

Godfrey, L. V., Herrera, C., Burr, G. S., Houston, J., Aguirre, I., & Jordan, T. E. (2021). δ13C and 14C activity of groundwater DOC and DIC in the volcanically active and arid Loa Basin of northern Chile. *Journal of Hydrology*, *595*, 125987.

Godfrey, L. V., Herrera, C., Burr, G. S., Houston, J., Aguirre, I., & Jordan, T. E. (2021). δ13C and 14C activity of groundwater DOC and DIC in the volcanically active and arid Loa Basin of northern Chile. *Journal of Hydrology*, *595*, 125987.

Gwalani, L. G., Rock, N. M. S., Chang, W. J., Fernandez, S., Allegre, C. J., & Prinzhofer, A. (1993). Alkaline rocks and carbonatites of Amba Dongar and adjacent areas, Deccan Igneous Province, Gujarat, India: 1. Geology, petrography and petrochemistry. *Mineralogy and Petrology*, *47*(2-4), 219-253.

Jay, A. E., & Widdowson, M. (2008). Stratigraphy, structure and volcanology of the SE Deccan continental flood basalt province: implications for eruptive extent and volumes. *Journal of the Geological Society*, *165*(1), 177-188.

Jinglu, W., Gagan, M. K., Xuezhong, J., Weilan, X., & Sumin, W. (2004). Sedimentary geochemical evidence for recent eutrophication of Lake Chenghai, Yunnan, China. *Journal of Paleolimnology*, *32*, 85-94.

Kaushal, R., Ghosh, P., & Pokharia, A. K. (2019). Stable isotopic composition of rice grain organic matter marking an abrupt shift of hydroclimatic condition during the cultural transformation of Harappan civilization. *Quaternary international*, *512*, 144-154.

Keller, G., Sahni, A., & Bajpai, S. (2009). Deccan volcanism, the KT mass extinction and dinosaurs. *Journal of biosciences*, *34*, 709-728.

Khosla, A., Kania, S., Lucas, S. G., & Verma, O. (2022). Charophytes from the Cretaceous–Palaeogene transition in the Jhilmili intertrappean beds of Central India. *Geological Journal*, *57*(11), 4412-4438.

Kim, S. T., & O'Neil, J. R. (1997). Equilibrium and nonequilibrium oxygen isotope effects in synthetic carbonates. *Geochimica et cosmochimica acta*, *61*(16), 3461-3475.

Liu, H., & Tang, X. (2022). Tongan volcanic eruption intensifies tropical cyclone Cody (2022). *Frontiers in Earth Science*, *10*, 904128.

Mandal, S., Bose, H., Ramesh, K., Sahu, R. P., Saha, A., Sar, P., & Kazy, S. K. (2022). Depth wide distribution and metabolic potential of chemolithoautotrophic microorganisms reactivated from deep continental granitic crust underneath the Deccan Traps at Koyna, India. *Frontiers in Microbiology*, *13*, 1018940.

Oza, H., Padhya, V., Ganguly, A., Saikranthi, K., Rao, T. N., & Deshpande, R. D. (2020). Hydrometeorological processes in semi-arid western India: insights from long term isotope record of daily precipitation. *Climate dynamics*, *54*, 2745-2757.

Paul, V., Banerjee, Y., Ghosh, P., & Busi, S. B. (2020). Depthwise microbiome and isotopic profiling of a moderately saline microbial mat in a solar saltern. *Scientific Reports*, *10*(1), 20686.

Petersen, S. V., Dutton, A., & Lohmann, K. C. (2016). End-Cretaceous extinction in Antarctica linked to both Deccan volcanism and meteorite impact via climate change. *Nature communications*, *7*(1), 12079.

Petersen, S.V., Defliese, W.F., Saenger, C., Daëron, M., Huntington, K.W., John, C.M., Kelson, J.R., Bernasconi, S.M., Colman, A.S., Kluge, T. and Olack, G.A. (2019). Effects of improved 17O correction on interlaboratory agreement in clumped isotope calibrations, estimates of mineral-specific offsets, and temperature dependence of acid digestion fractionation. *Geochemistry, Geophysics, Geosystems*, *20*(7), 3495-3519.

Rajala, P., & Bomberg, M. (2017). Reactivation of deep subsurface microbial community in response to methane or methanol amendment. *Frontiers in Microbiology*, *8*, 243735.

Rangarajan, R., Pathak, P., Banerjee, S., & Ghosh, P. (2021). Floating boat method for carbonate stable isotopic ratio determination in a GasBench II peripheral. Rapid Communications in Mass Spectrometry, 35(15), e9115

Ray, J. S., & Ramesh, R. (1999). Evolution of carbonatite complexes of the Deccan flood basalt province: Stable carbon and oxygen isotopic constraints. *Journal of Geophysical Research: Solid Earth*, *104*(B12), 29471-29483.

Ray, J. S., Pande, K., & Pattanayak, S. K. (2003). Evolution of the Amba Dongar Carbonatite Complex: Constraints from 40Ar-39Ar chronologies of the Inner Basalt and an alkaline plug. *International Geology Review*, *45*(9), 857-862.

Renne, P. R., Sprain, C. J., Richards, M. A., Self, S., Vanderkluysen, L., & Pande, K. (2015). State shift in Deccan volcanism at the Cretaceous-Paleogene boundary, possibly induced by impact. *Science*, *350*(6256), 76-78.

Sahu, R. P., Kazy, S. K., Bose, H., Mandal, S., Dutta, A., Saha, A., ... & Sar, P. (2022). Microbial diversity and function in crystalline basement beneath the Deccan Traps explored in a 3 km borehole at Koyna, western India. *Environmental Microbiology*, *24*(6), 2837-2853.

Samant, B., Kumar, D., Mohabey, D. M., Kapgate, D. K., Manchester, S. R., & Patil, S. K. (2020)[a]. Palynoflora from intertrappean localities in southeastern part of Deccan volcanic province: taxonomic composition, age and paleogeographic implications. *Palaeoworld*, *29*(1), 161-175.

Samant, Bandana, Kumar, Arun, Mohabey, D.M., Humane, Sumedh, Kumar, Deepesh, Dhoble, Anup, and Pizal, Priya. (2020)[b]. Centropyxis aculeata (testate lobose amoebae) and associated diatoms from the intertrappean lacustrine sediments (Maastrichtian) of central India: implications in understanding paleolake ecology. Palaeontologia Electronica, 23(3):a60. https://doi.org/10.26879/1082

Samant, B., Puranik, S., Kapgate, D. K., Mohabey, D. M., & Dhobale, A. (2022). Palynoflora from an Upper Cretaceous freshwater paleolake in central India: paleoecological implications. *Cretaceous Research*, *139*, 105302.

Samal, A. K., Srivastava, R. K., & Upadhyay, D. (2021). Major, trace, and rare-earth element geochemistry of Nb-V rich Andradite-Schorlomite-Morimotoite Garnet from Ambadungar-Saidivasan alkaline carbonatite complex, India: Implication for the role of hydrothermal fluid-induced metasomatism. Minerals, 11(7), 756.

Schoene, Blair, Kyle M. Samperton, Michael P. Eddy, Gerta Keller, Thierry Adatte, Samuel A. Bowring, Syed FR Khadri, and Brian Gertsch. (2015). "U-Pb geochronology of the Deccan Traps and relation to the end-Cretaceous mass extinction." *Science* 347, 6218,182-184.

Self, S., Mittal, T., Dole, G., & Vanderkluysen, L. (2022). Toward understanding Deccan volcanism. *Annual Review of Earth and Planetary Sciences*, *50*, 477-506.

Simonetti, A., Bell, K., & Viladkar, S. G. (1995). Isotopic data from the Amba Dongar carbonatite complex, west-central India: evidence for an enriched mantle source. *Chemical Geology*, *122*(1-4), 185-198.

Singh, T., Upadhyay, D., Patel, A. K., & Mishra, B. (2022). High MREE-HREE solubility in a carbonatite-derived hydrothermal fluid: Evidence from fluorite-hosted fluid inclusions in the Amba Dongar carbonatite complex, India. *Chemical Geology*, *613*, 121162.

Srivastava, R. K. (1997). Petrology, geochemistry and genesis of rift-related carbonatites of Ambadungar, India. *Mineralogy and Petrology*, *61*(1-4), 47.

Tandon, S. K. (2002). Records of the influence of Deccan volcanism on contemporary sedimentary environments in Central India. *Sedimentary Geology*, *147*(1-2), 177-192.

Tandon, S. K., & Andrews, J. E. (2001). Lithofacies associations and stable isotopes of palustrine and calcrete carbonates: examples from an Indian Maastrichtian regolith. *Sedimentology*, *48*(2), 339-355.

Tandon, S. K., Sood, A., Andrews, J. E., & Dennis, P. F. (1995). Palaeoenvironments of the dinosaur-bearing lameta beds (Maastrichtian), Narmada valley, central India. *Palaeogeography, Palaeoclimatology, Palaeoecology*, *117*(3-4), 153-184.

Templeton, A. S., & Caro, T. A. (2023). The rock-hosted biosphere. *Annual Review of Earth and Planetary Sciences*, *51*, 493-519.

Teranes, J. L., McKenzie, J. A., Lotter, A. F., & Sturm, M. (1999). Stable isotope response to lake eutrophication: Calibration of a high-resolution lacustrine sequence from Baldeggersee, Switzerland. *Limnology and Oceanography*, *44*(2), 320-333.

Tobin, T. S., Bitz, C. M., & Archer, D. (2017). Modeling climatic effects of carbon dioxide emissions from Deccan Traps volcanic eruptions around the Cretaceous–Paleogene boundary. *Palaeogeography, Palaeoclimatology, Palaeoecology*, *478*, 139-148.

Usdowski, E., & Hoefs, J. (1993). Oxygen isotope exchange between carbonic acid, bicarbonate, carbonate, and water: a re-examination of the data of McCrea (1950) and an expression for the overall partitioning of oxygen isotopes between the carbonate species and water. *Geochimica et Cosmochimica Acta*, *57*(15), 3815-3818.

Usdowski, E., Michaelis, J., Böttcher, M.E. and Hoefs, J., 1991. Factors for the oxygen isotope equilibrium fractionation between aqueous and gaseous CO2, carbonic acid, bicarbonate, carbonate, and water (19 C). *Z. Phys. Chem*, *170*, pp.237-249.

Viladkar, S. G. (1981). The carbonatites of Amba Dongar, Gujarat, India. *Bull. Geol. Soc. Finland*, *53*(1), 17-28.

Viladkar, S. G. (2015). Mineralogy and Geochemistry of fenitized nephelinites of the Amba Dongar Complex, Gujarat. *Journal of the Geological Society of India*, *85*(1), 87-97.

Viladkar, S. G., & Sorokhtina, N. V. (2021). Evolution of pyrochlore in carbonatites of the Amba Dongar complex, India. *Mineralogical Magazine*, *85*(4), 554-567.

Viladkar, S. G., & Sorokhtina, N. V. (2021). Evolution of pyrochlore in carbonatites of the Amba Dongar complex, India. *Mineralogical Magazine*, *85*(4), 554-567.

Viladkar, S. G., Ramesh, R., Avasia, R. K., & Pawaskar, P. B. (2005). Extrusive Phase of Carbonatite-Alkalic Activity in Amba Dongar Complex, Chhota Udaipur, Gujarat. *Geological Society of India*, *66*(3), 273-276.

Zaarur, S., Affek, H. P., & Brandon, M. T. (2013). A revised calibration of the clumped isotope thermometer. *Earth and Planetary Science Letters*, *382*, 47-57.

Zhang, L., Wang, C., Wignall, P. B., Kluge, T., Wan, X., Wang, Q., & Gao, Y. (2018). Deccan volcanism caused coupled pCO2 and terrestrial temperature rises, and pre-impact extinctions in northern China. *Geology*, *46*(3), 271-274.

Figures

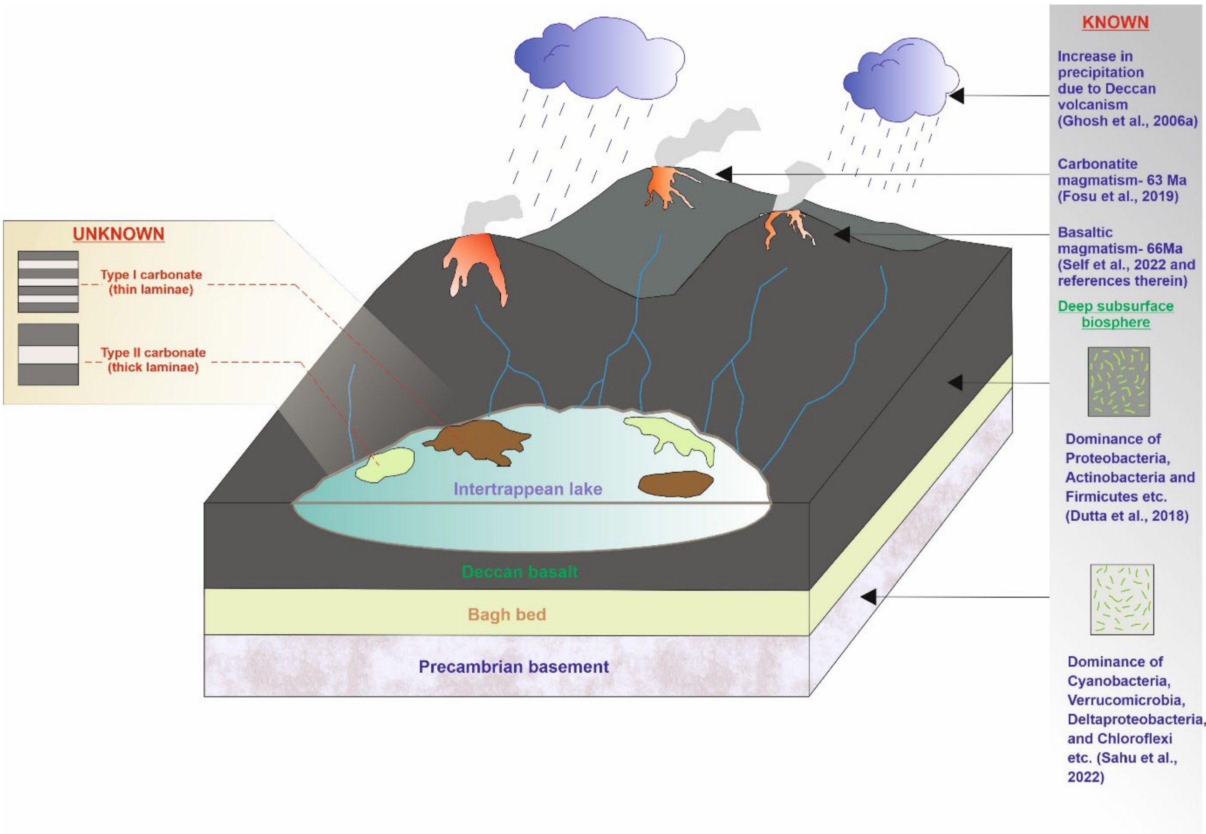

Figure 1| Graphic representation of the regional geological and geomicrobiological background ("Known") and highlighting the motivation of the project ("Unknown"). Previous investigations showed that the Deccan volcanism peaked around 66 Ma (Self et al., 2022 and references therein). U-Pb dates yielded a mean age of 63 Ma for the carbonatite magmatism from the Amba Dongar region (Fosu et al. 2019). Oxygen isotope investigation on the intertrappean bole bed clays captured evidence of the intensification of rainfall related to the Deccan volcanism (Ghosh et al., 2004). Geomicrobiological investigations on the samples retrieved from the Koyna deep scientific drilling project provided insights into the subsurface microbiome from the Deccan basalt (Dutta et al., 2018) and Granitic basement (Sahu et al., 2022).

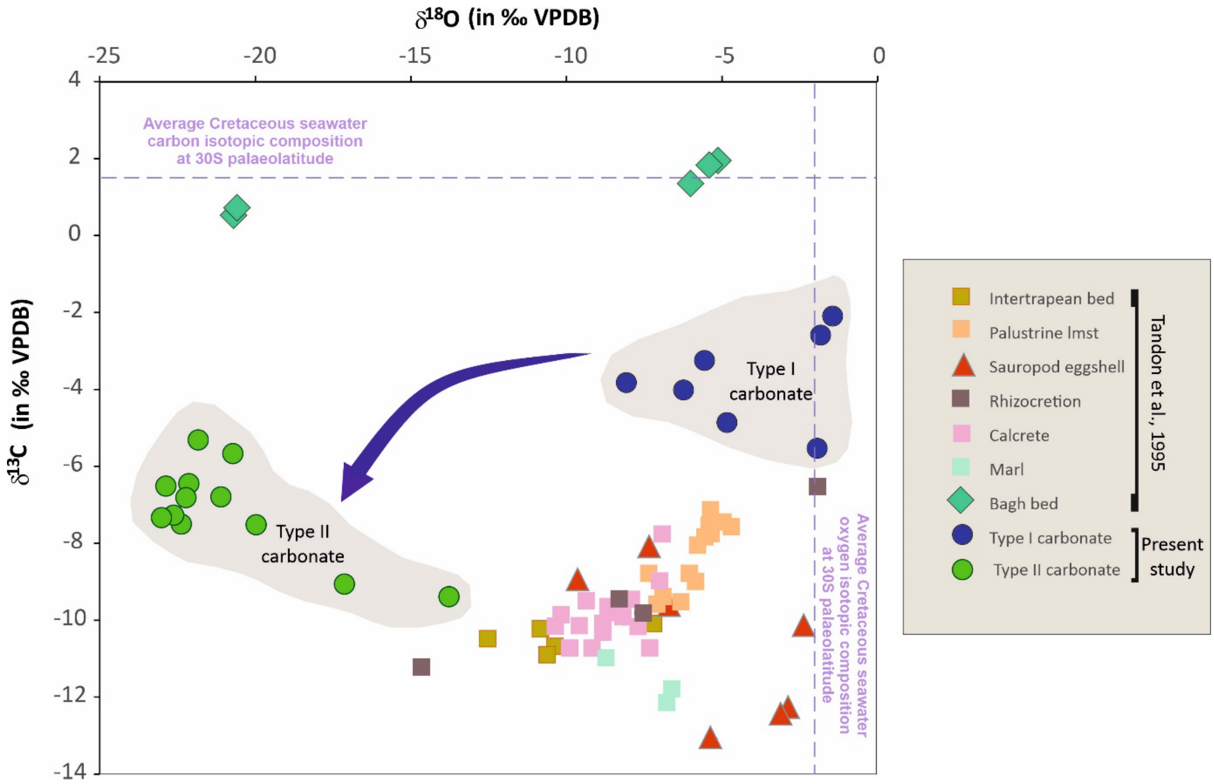

Figure 2| Stable carbon and oxygen isotopic compositions of Type I (blue circle) and Type II microbial? carbonates investigated in the present study. A comparison of stable isotope record of cretaceous carbonate of multiple origin documented from the region nearby and also intertrappean carbonates (Tandon et al., 1995) together with average Cretaceous seawater composition at 30S palaeolatitude (Ghosh et al., 2018) showed a district compositional shift in case of oxygen isotopes recording a large change in environmental condition from marine to continental settings (shown by arrow).

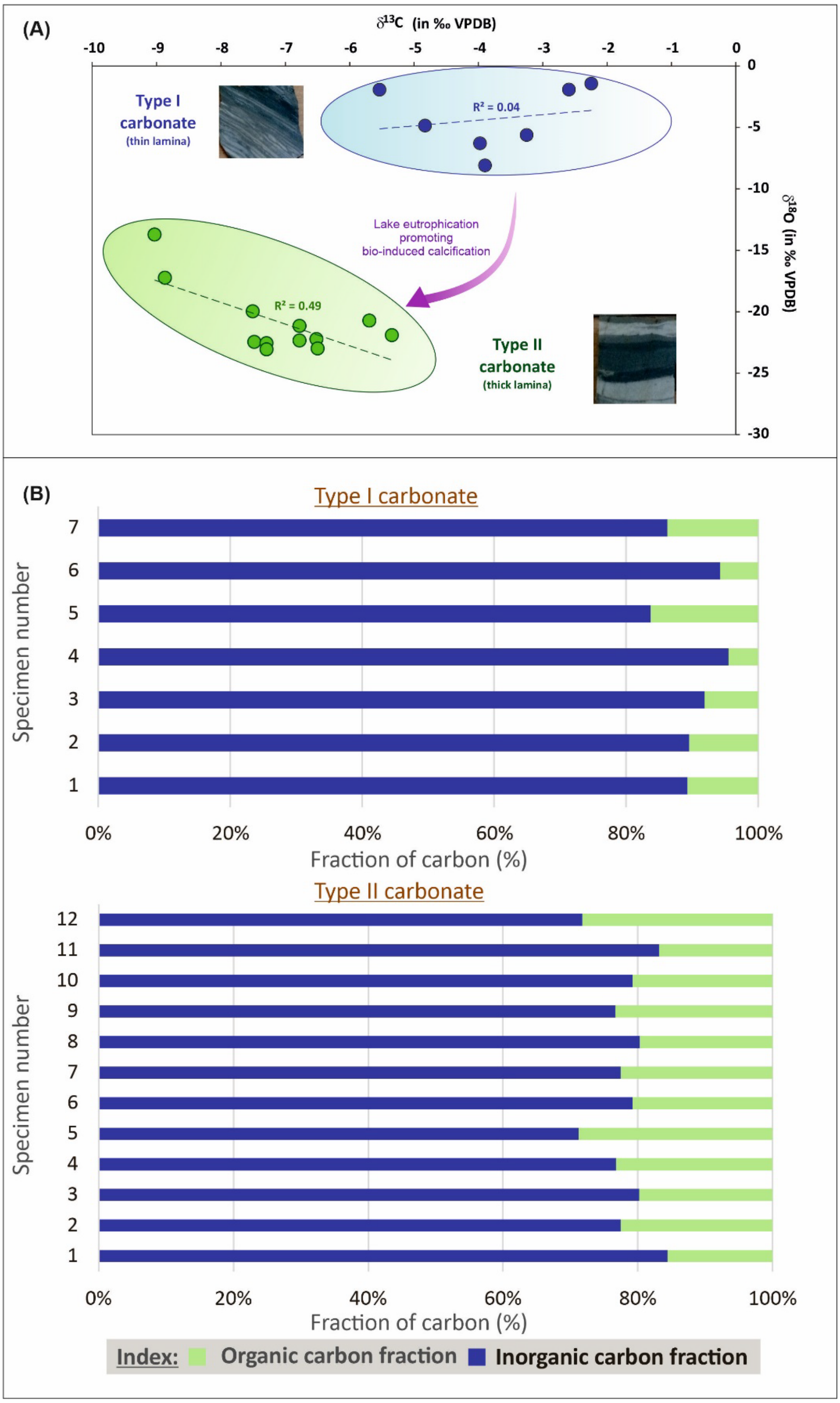

Figure 3| (A) $\delta^{13}C$ vs $\delta^{18}O$ cross-plot for different types of carbonates analysed in this study. (B) Results from the two-component mixing model denoting contribution of dissolved inorganic carbon from the oxidation of organics present in the environment.

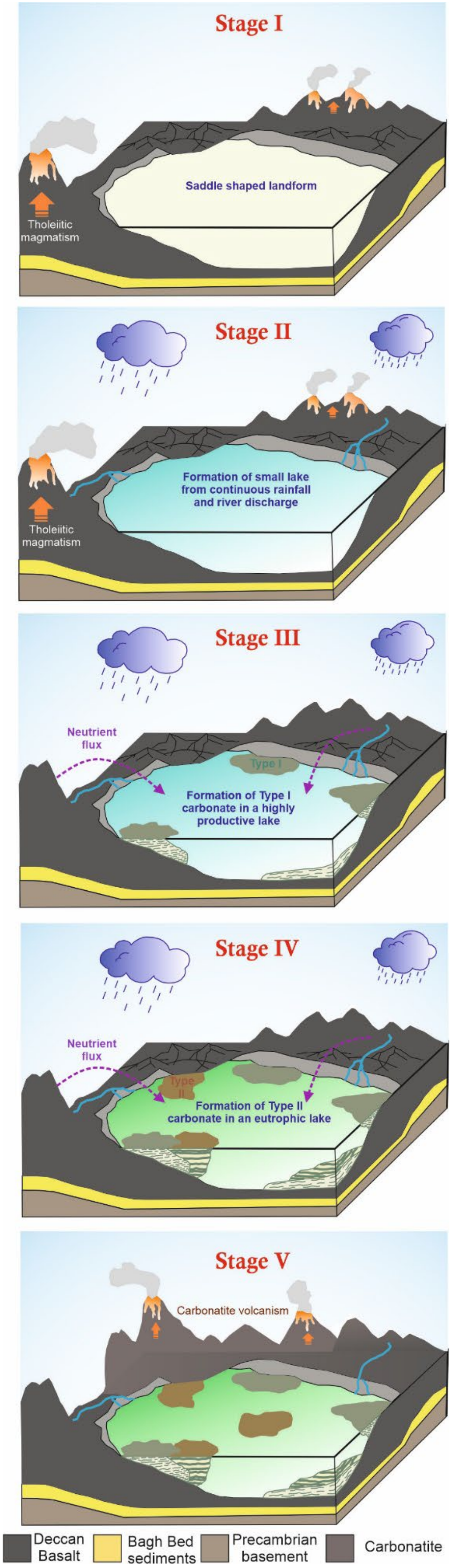

Figure 4| Schematic representation of different stages of lake evolution and formation of both types of carbonates accordingly.

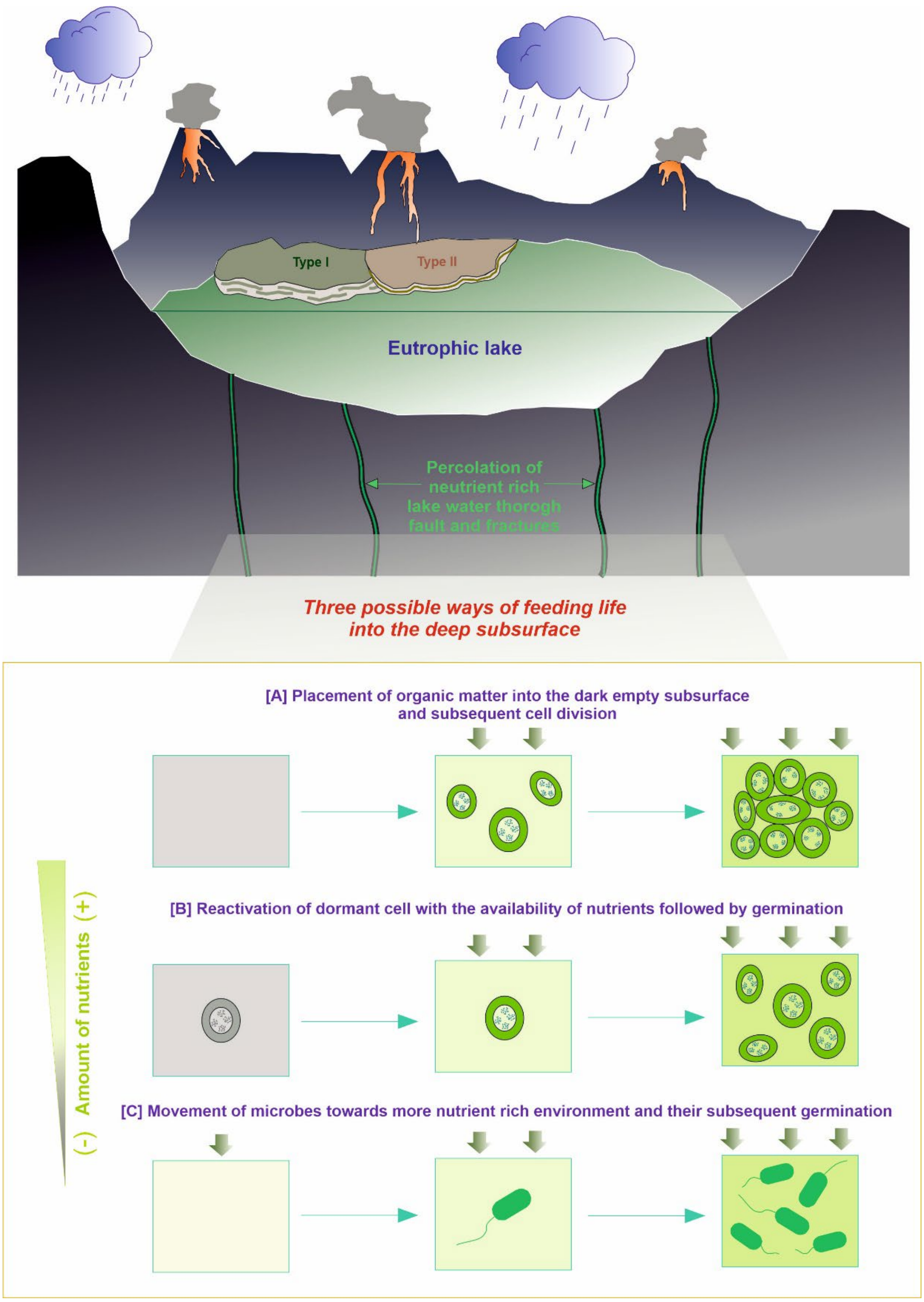

Figure 5| Conceptual model explaining the possibilities for nutrient-rich intertrappean lake water to promote deep microbial biosphere within the Deccan trap.

<u>**Supplementary Information**</u>

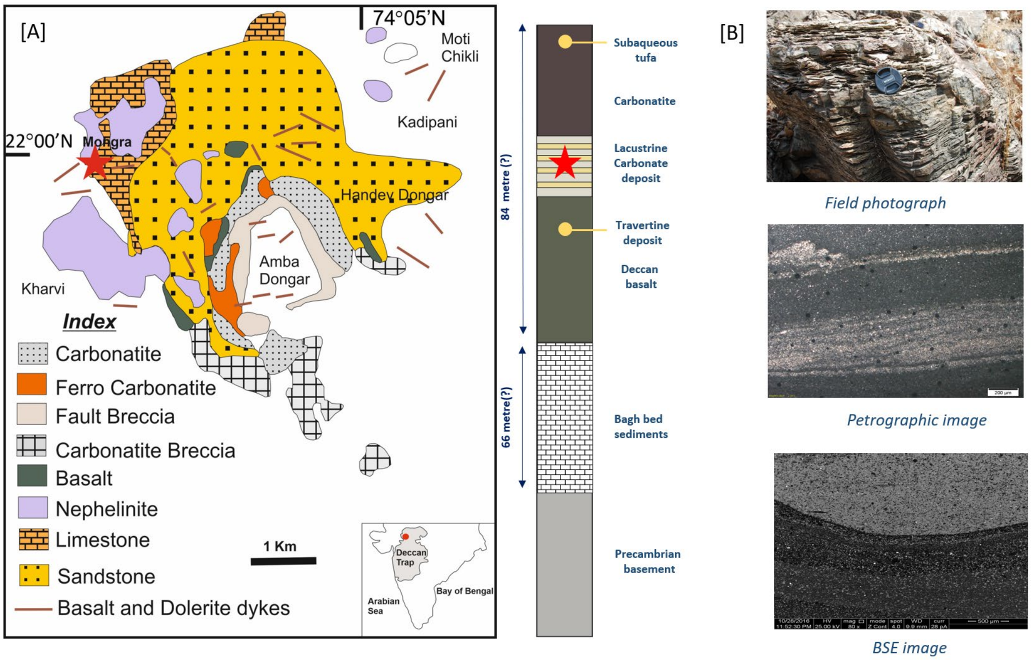

Supplementary Figure S1: (A) Geological map of Amba Dongar carbonatite complex (modified from Viladkar 2015). The red star marks the location for lacustrine carbonate occurrences investigated in the present study. Generalized stratigraphy for the region constructed based on the Geological Survey of India and SPG reports (Gopinath 1970, Ray 1981) is schematically shown in the stratigraphic column. (B) Panel B shows outcrop photographs of the microbial carbonates. (D) Petrographic thin section image of the carbonate. (E) BSE image of the section showing distinct laminations.

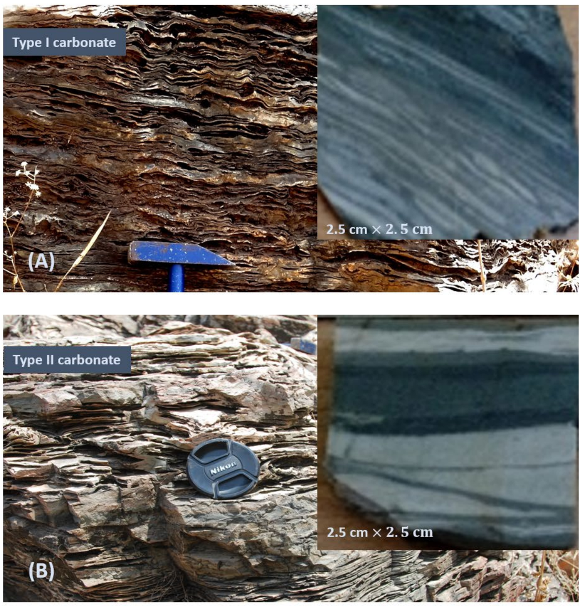

Supplementary Figure S2: Field and thick section photographs of Type I (A) and Type II microbial carbonates (B) investigated in the present study.

3D imagery of microbialites:

An X-ray-based μCT scanning method has been demonstrated to be an important tool for the 3D reconstruction of microbially induced sedimentary deposits and for interpreting environment-biota interactions (Howard et al., 2024). In our study we have used this technique to understand the microbialite taphonomy.

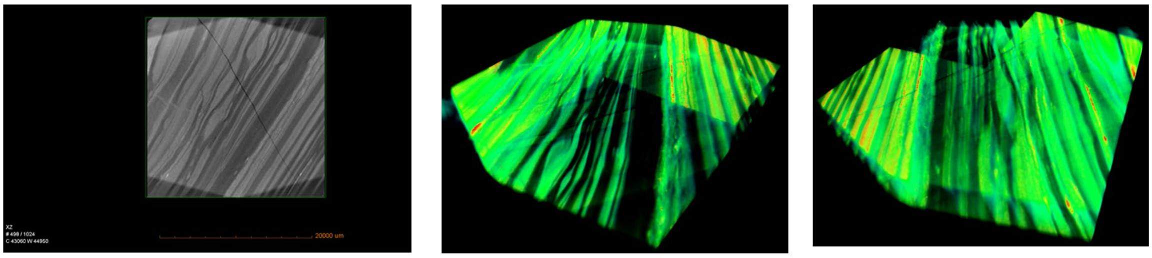

Supplementary Figure S3 (A): Micro-computed tomography (μCT) of the laminae from Type I microbial carbonates obtained using ZEISS XRADIA.

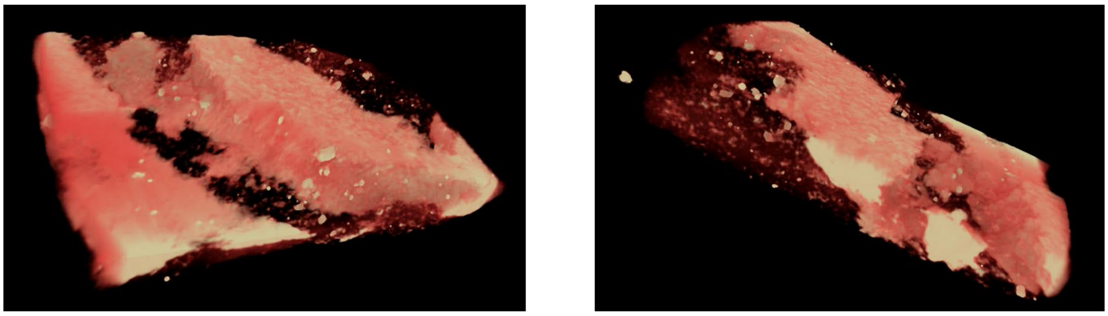

Supplementary Figure S3 (B): Micro-computed tomography (μCT) of the laminae from Type II microbial carbonates obtained using ZEISS XRADIA. The section was taken near the contact metamorphic zone (Fig. S5) where calcite was transformed into the wollastonite. The 3D tomographic reconstruction shows the presence of microbial chip (white arrow) originating from the destabilization of the mat environment with the pulses of carbonatite volcanism.

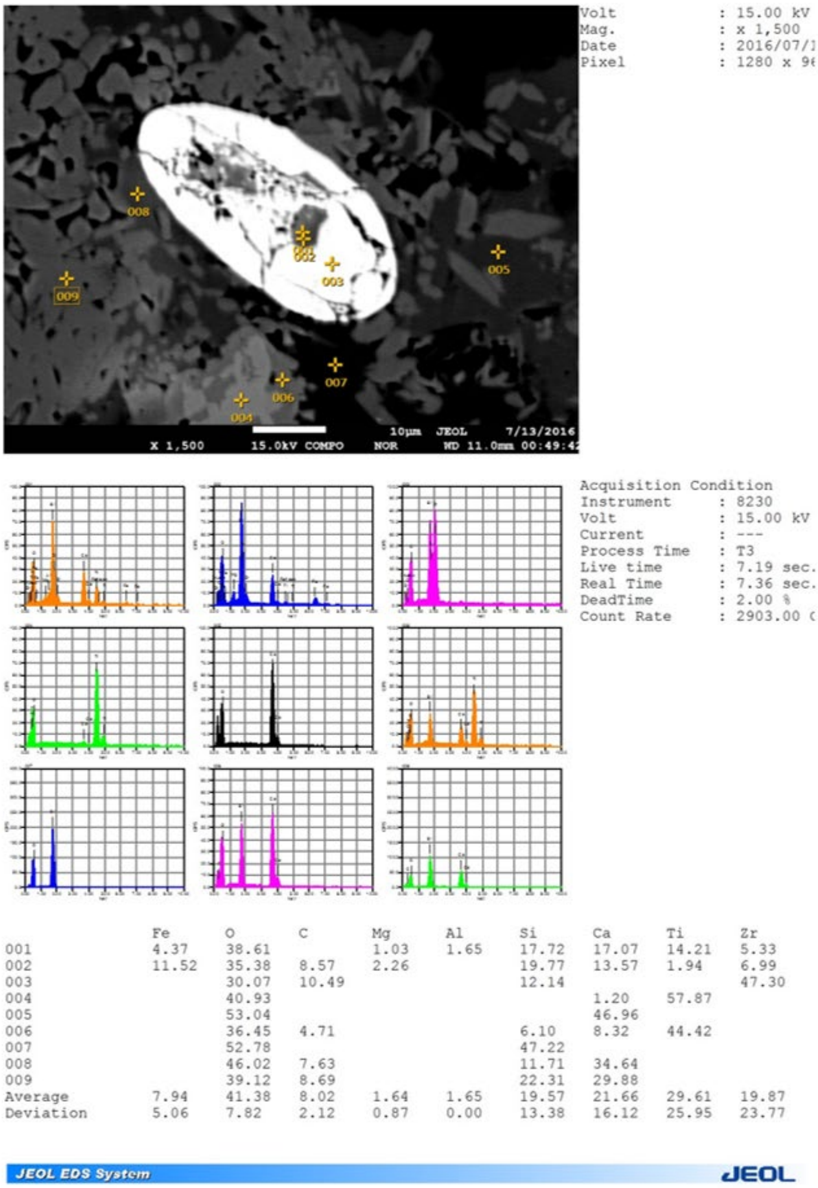

	Fe	O	C	Mg	Al	Si	Ca	Ti	Zr
001	4.37	38.61		1.03	1.65	17.72	17.07	14.21	5.33
002	11.52	35.38	8.57	2.26		19.77	13.57	1.94	6.99
003		30.07	10.49			12.14			47.30
004		40.93					1.20	57.87	
005		53.04					46.96		
006		36.45	4.71			6.10	8.32	44.42	
007		52.78				47.22			
008		46.02	7.63			11.71	34.64		
009		39.12	8.69			22.31	29.88		
Average	7.94	41.38	8.02	1.64	1.65	19.57	21.66	29.61	19.87
Deviation	5.06	7.82	2.12	0.87	0.00	13.38	16.12	25.95	23.77

Supplementary Figure S4: BSE image and EDS analysis showing the presence of detrital zircon grains suggesting riverine mode for the transportation and deposition into the environment and accommodating in the microbial carbonate growth.

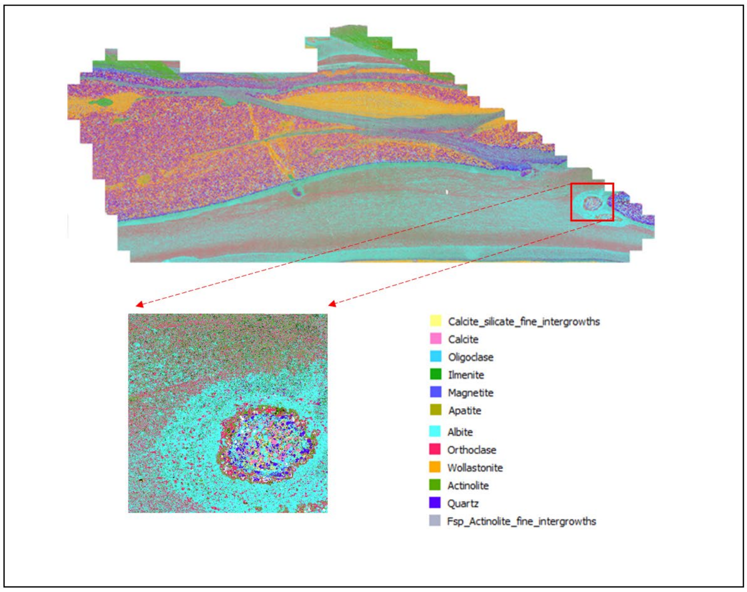

Supplementary Figure S5: Different mineral phases present in Type II carbonate were revealed using a TIMA-based investigation. Here we found presence of metasomatic minerals suggesting fluid action and hydrothermal input.

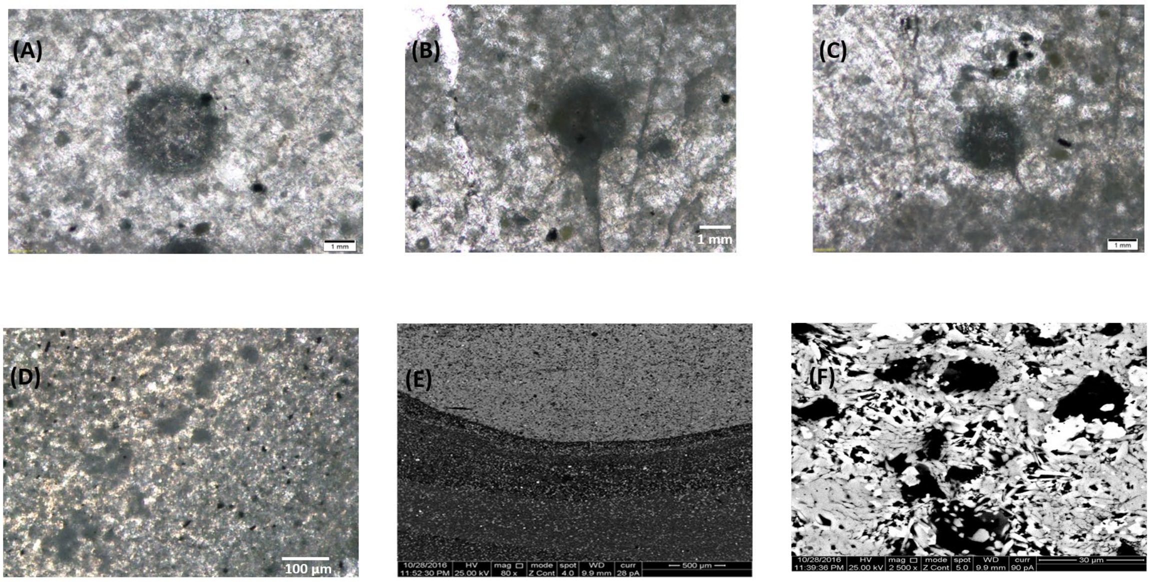

Supplementary Figure S6: (A) Photomicrograph of Ooid with relict radial fabric at the rim with evidence of micritization. The dark patches probably resulted from the activity of endolithic algae. (B) and (C) Flagella(/tail)- like structures, possibly indicating the motility of microorganisms. (D) Micrite with clotted texture capturing evidence of microbially induced precipitation. (E) BSE image of the section showing distinct laminations. (F) BSE image showing the presence of peloid microspar-like structure developed by heterotrophic bacterial activity.

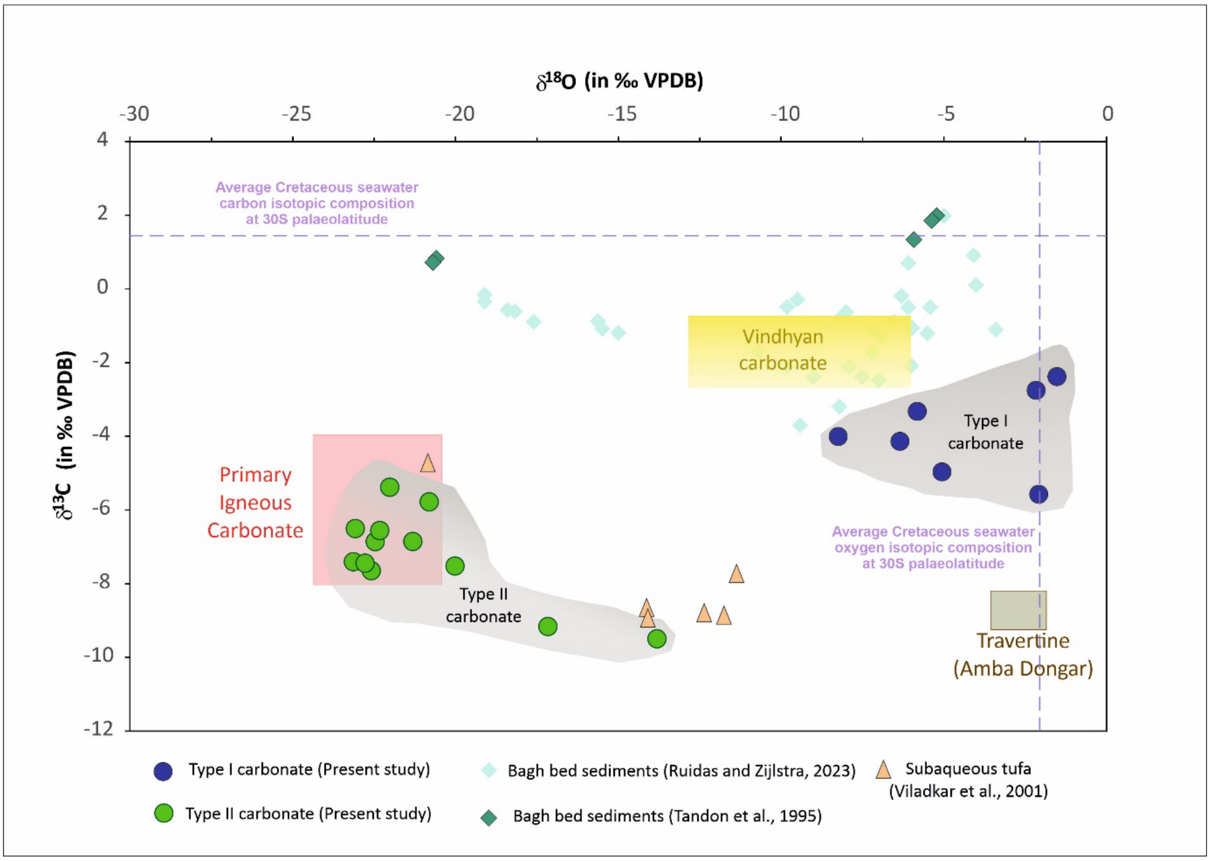

Supplementary Figure 7: Stable isotope composition of the lacustrine carbonates (Type I and II) are compared with the other contemporary local carbonate bodies: Primary Igneous carbonate field (Fosu et al., 2020 and references therein); Bagh bed carbonates (Tandon et al., 1995; Ruidas and Zijlstra 2023); local Proterozoic carbonate -Vindhyan carbonate (Banerjee et al., 2007); travertine from Amba Dongar (present study); post carbonatite subaqueous tufa from Amba Dongar (Viladkar et al., 2001). Average cretaceous seawater composition at 30°S palaeolatitude (Ghosh et al., 2018) was also marked by the purple line.

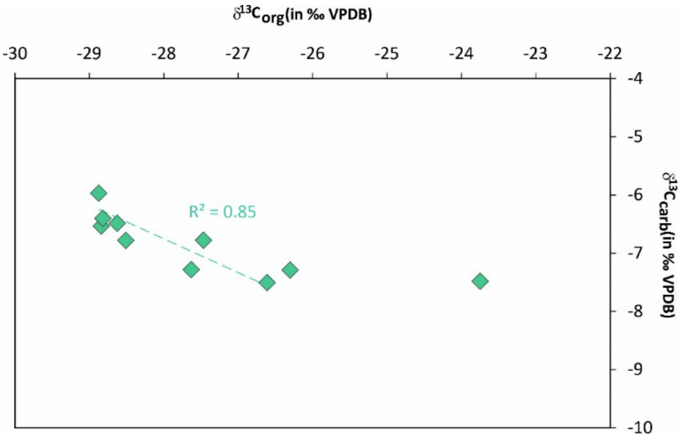

Supplementary Figure S8: $\delta^{13}C_{org}$ vs $\delta^{13}C_{carb}$ correlation for the Type II carbonates investigated in this study.

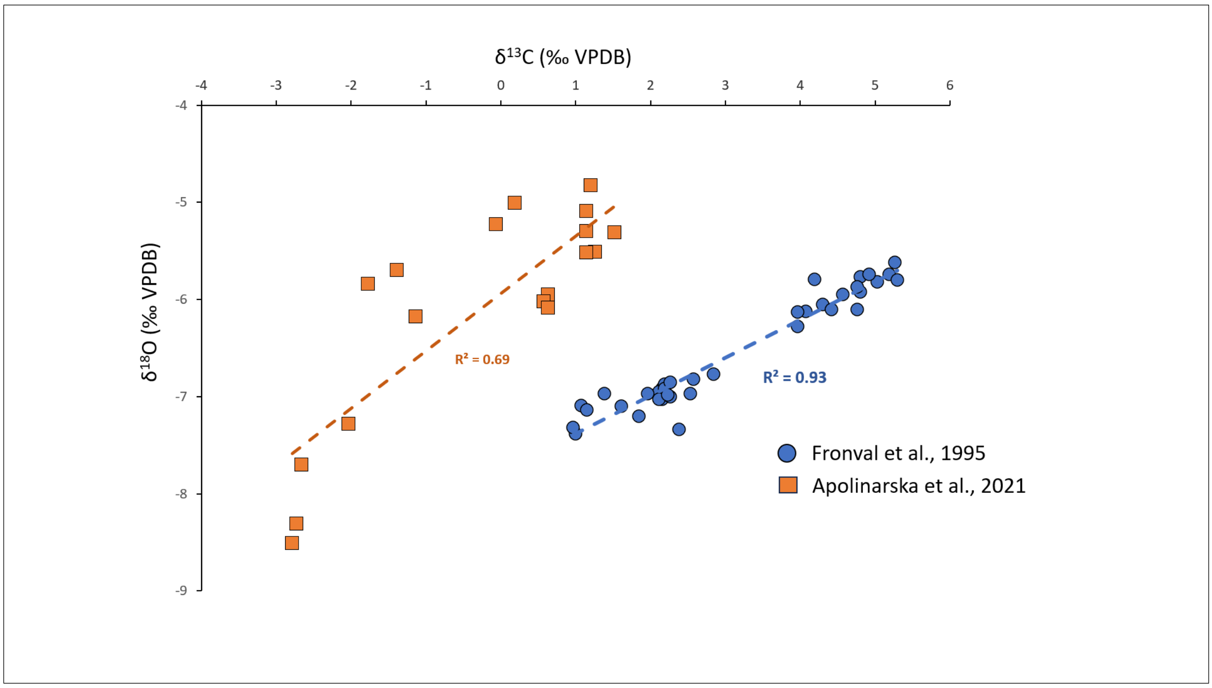

Supplementary Figure S9: $\delta^{13}C$ vs $\delta^{18}O$ cross plots showing a high correlation for the bio-induced carbonate precipitated in modern Lake Kierskie (Apolinarska et al., 2021) and Lake Arresù (Fronval et al., 1995) during eutrophication.

References:

Apolinarska, K., Pleskot, K., Pełechata, A., Migdałek, M., & Pełechaty, M. (2021). Seasonal deposition of authigenic calcite out of isotopic equilibrium with DIC and water, and implications for paleolimnological studies. *Journal of Paleolimnology*, *66*(1), 41-53.

Banerjee, S., Bhattacharya, S. K., & Sarkar, S. (2007). Carbon and oxygen isotopic variations in peritidal stromatolite cycles, Paleoproterozoic Kajrahat Limestone, Vindhyan basin of central India. *Journal of Asian Earth Sciences*, *29*(5-6), 823-831.

Fronval, T., Bo Jensen, N., & Buchardt, B. (1995). Oxygen isotope disequilibrium precipitation of calcite in Lake Arresø, Denmark. *Geology*, *23*(5), 463-466.

Ghosh, P., Prasanna, K., Banerjee, Y., Williams, I. S., Gagan, M. K., Chaudhuri, A., & Suwas, S. (2018). Rainfall seasonality on the Indian subcontinent during the cretaceous greenhouse. Scientific Reports, 8(1), 1–9.

Gopinath, K. (1972). Geological mapping in parts of Baroda and Broach districts, Gujarat. Progress report for the field season 1970-71, Geological Survey of India.

Howard, C. M., Sheldon, N. D., Smith, S. Y., & Noffke, N. (2024). Interpreting an Archaean paleoenvironment through 3D imagery of microbialites. *Geobiology*, *22*(3), e12601.

Ray, D. (1981). Stratigraphy and sedimentation of the Bagh Beds of Lower Narmada valley, Gujarat. *Unpublished PhD thesis). The Maharaja Sayajirao University of Baroda, Vadodara*.

Ruidas, D. K., & Zijlstra, J. J. P. (2023). The hardgrounds of the Turonian–Coniacian carbonates of the Bagh Group of central India. *Journal of Earth System Science*, *132*(1), 27.

Tandon, S. K., Sood, A., Andrews, J. E., & Dennis, P. F. (1995). Palaeoenvironments of the dinosaur-bearing lameta beds (Maastrichtian), Narmada valley, central India. *Palaeogeography, Palaeoclimatology, Palaeoecology*, *117*(3-4), 153-184.

Viladkar, S. G. (1981). The carbonatites of Amba Dongar, Gujarat, India. *Bull. Geol. Soc. Finland*, *53*(1), 17-28.